International Journal of Applied Science and Engineering Review

IJASER

ISSN: 2582-6271

Vol. 6, Issue. 6, Nov-Dec 2025, page no. 64-74

To cite this article: Nur Rokhati, Asep Muhamad Samsudin*, Widyah Anggraini (2025). PURIFICATION OF GLUCOSAMINE THROUGH COOLING CRYSTALLIZATION, International Journal of Applied Science and Engineering Review (IJASER) 6 (6): 64-74 Article No. 252 Sub Id 378

PURIFICATION OF GLUCOSAMINE THROUGH COOLING CRYSTALLIZATION

Nur Rokhati, Asep Muhamad Samsudin*, Widyah Anggraini

Department of Chemical Engineering, Faculty of Engineering, Universitas Diponegoro, Semarang 50275, Indonesia
Membrane Research Center, Integrated Laboratory for Research and Services, Universitas Diponegoro, Semarang 50275, Indonesia
*Corresponding author: asep.samsudin@live.undip.ac.id

DOI: https://doi.org/10.52267/IJASER.2025.6605

ABSTRACT

Glucosamine (GlcN, 2-amino-2-deoxy-D-glucose) is an amino sugar and a key structural component of cartilage, commonly produced from animal sources, microbial fermentation, and fungi. Owing to its extensive applications in osteoarthritis treatment, dietary supplements, and cosmetic formulations, achieving high glucosamine purity is essential. This study investigates the purification of glucosamine using cooling crystallization, a method that induces supersaturation through controlled temperature reduction. Optimal crystallization was achieved from a saturated feed solution at 0 °C under 500 rpm agitation for 6 h. SEM analysis showed that the obtained crystals exhibited smooth and compact morphology. FTIR analysis confirmed the presence of characteristic functional groups, including O–H (3283 cm^{-1}), N–H (1657.97 cm^{-1}), and C–N (1154.28 cm^{-1}). HPLC analysis yielded a retention time of 1.962 min, indicating successful purification. These results demonstrate that cooling crystallization is an effective and straightforward technique for producing high-quality glucosamine suitable for pharmaceutical and cosmetic applications.

KEYWORDS: glucosamine, crystallization, cooling

1. INTRODUCTION

Glucosamine (GlcN, 2-amino-2-deoxy-D-glucose) is an amino sugar naturally present in the human body and functions as a fundamental structural component of cartilage. Glucosamine units polymerize to form glycosaminoglycans, which constitute essential carbohydrate chains in connective tissues. These chains subsequently assemble into proteoglycans that bind to core proteins and play critical roles in regulating cell growth and differentiation [1].

ISSN: 2582-6271

Vol. 6, Issue.6, Nov-Dec 2025, page no. 64-74

Glucosamine is widely applied in the health sector, particularly in osteoarthritis therapeutics, dietary supplements, and cosmetic formulations designed to enhance skin condition. Its broad functional benefits and commercial relevance have increased the demand for high-quality glucosamine products. Consequently, the development of efficient, scalable, and cost-effective glucosamine production and purification methods has attracted substantial research interest [2].

Glucosamine is commonly produced from chitin, a natural polysaccharide composed of N-acetylglucosamine units linked through β(1→4) glycosidic bonds [2]. Chitin deacetylation generates chitosan, which serves as an intermediate substrate for glucosamine production. Chitosan is a copolymer of N-acetylglucosamine (GlcNAc) and β(1→4)-2-amino-2-deoxy-D-glucopyranose (GlcN), typically containing more than 50% glucosamine units. Chitosan can be hydrolyzed using hydrochloric acid or degraded by Serratia marcescens KAHN 15.12 to yield glucosamine hydrochloride and N-acetylglucosamine [3].

GlcN can also be produced through the enzymatic hydrolysis of chitosan using enzymes such as cellulase, pectinase, pepsin, papain, neutral proteases, lipases, and α-amylase [4]. This enzymatic approach offers notable advantages, including high substrate specificity and high product yield, while maintaining the integrity of the glucose ring structure [5]. However, the hydrolysate obtained from this process generally remains in solution form and contains various impurities. Therefore, additional purification steps are required to obtain glucosamine of suitable quality for further applications.

One of the purification methods currently being explored for glucosamine production is purification via crystallization. Crystallization involves the formation of solid crystals from a solution as it undergoes heating, saturation, cooling, and subsequent precipitation [6]. This technique is frequently selected due to its cost-effectiveness and suitability for large-scale purification. In this process, supersaturation plays a critical role, as it governs the initiation of crystal nucleation and significantly influences the subsequent crystal growth dynamics [7].

Various crystallization techniques have been developed, among which cooling crystallization is widely favored due to its simplicity and ability to produce high-quality crystals [8]. This method has been applied in several studies, including saturation simulation and feedback-controlled semi-batch cooling crystallization investigations on the influence of mixing on the size distribution of borax decahydrate crystals in batch cooling crystallization [9], and the crystallization of patchouli alcohol from patchouli oil [5]. Therefore, the present study aims to evaluate the crystallization performance of the cooling crystallization method for the purification of glucosamine.

International Journal of Applied Science and Engineering Review

IJASER

ISSN: 2582-6271

Vol. 6, Issue.6, Nov-Dec 2025, page no. 64-74

2. METHODS

2.1 Materials

The materials used in this study included glucosamine obtained from Sigma-Aldrich (CAS No. 66-84-2) and distilled water.

2.2 Crystallization Process

Figure 1 shows the crystallization equipment used in this study. Glucosamine solutions were prepared at concentrations of 45% w/v (supersaturated) and 21% w/v (unsaturated). Each solution was transferred into a saturator tank (4) and maintained at 60 °C until reaching saturation, which was confirmed when additional glucosamine no longer dissolved. The saturated solutions were stirred at 300, 400, or 500 rpm and subsequently directed to a cooling tank (5), where the temperature (3) was controlled at either 0 °C or 25 °C for cooling periods of 2, 4, or 6 h. After cooling, the suspensions were filtered using a vacuum filtration unit (7) to recover the glucosamine crystals, which were then collected and weighed.

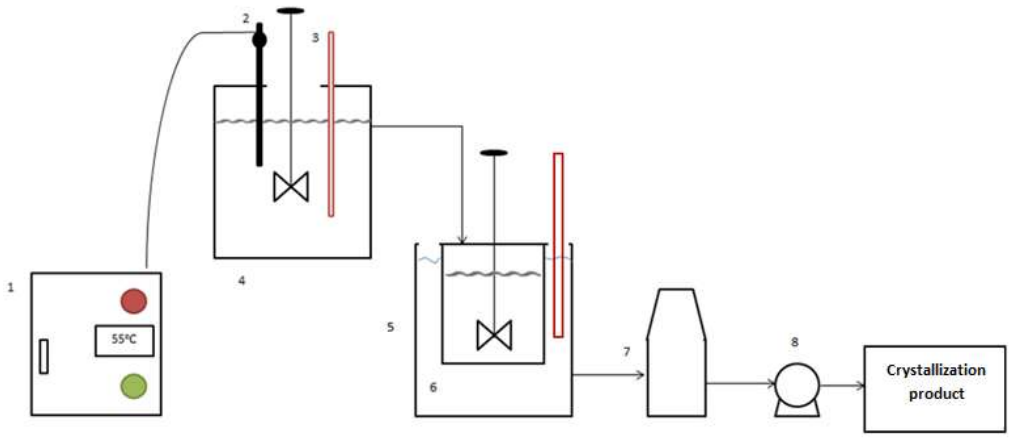

Figure 1: Crystallization equipment: (1) Temperature controller, (2) Thermocouple, (3) Thermometer, (4) Saturator tank, (5) Cooling tank, (6) Cooling water, (7) Slurry tank, and (8) Vacuum filter.

2.3 Yield Measurement

Product yield was calculated based on the mass of crystals recovered relative to the initial material used. The percentage yield was determined using Equation (1):

$$Yield\ (\%) = \frac{Amount\ of\ material\ produced\ (g)}{Amount\ of\ material\ before\ processing\ (g)} \times 100\% \qquad (1)$$

International Journal of Applied Science and Engineering Review

IJASER

ISSN: 2582-6271

Vol. 6, Issue.6, Nov-Dec 2025, page no. 64-74

2.4 Characterization

Scanning Electron Microscopy (SEM) (JEOL JSM-6510LA) was performed to examine the surface morphology of glucosamine crystals before and after crystallization. Samples were dried, mounted on aluminum stubs, and sputter-coated with gold. Imaging was conducted at magnifications of 1,000×, 2,000×, 5,000×, and 10,000× to observe changes in crystal structure and compactness.

FTIR analysis (Perkin-Elmer UATR Spectrum Two) was performed to identify the functional groups present in the glucosamine crystals. Spectra were collected in the range of 4000–400 cm^{-1}. This analysis enabled the confirmation of characteristic vibrational bands associated with O–H, N–H, and C–N functional groups.

HPLC analysis (Shimadzu LC-20AD) was performed to determine the purity and retention time of the crystallized glucosamine. Samples were filtered through a 0.45 µm membrane prior to injection. Separation was conducted using a C18 column under isocratic elusion, with the mobile phase and flow rate set according to standard glucosamine analysis conditions. Detection was carried out using a UV detector, and retention time values were used to evaluate the effectiveness of the purification process.

3. RESULTS AND DISCUSSION

3.1 Effect of Glucosamine Concentration on Purification Through Cooling Crystallization

In this study, the crystallization behavior of glucosamine was evaluated by comparing saturated and unsaturated solutions. In the saturated solution containing 45% w/v glucosamine, crystal formation was observed at cooling times of 2, 4, and 6 hours, with the yield increasing progressively as the cooling duration increased. In contrast, no crystalline product was obtained from the 21% w/v solution because the glucosamine powder continued to dissolve in distilled water, resulting in a homogeneous unsaturated solution.

Crystal formation in the supersaturated solution occurred because supersaturation is a primary driving force for both nucleation and crystal growth. Under supersaturated conditions, the system initiates the formation of crystal nuclei and subsequently promotes their growth into larger crystals. Nucleation is triggered when supersaturation develops, typically due to solvent separation or a reduction in solution temperature [10].

In the unsaturated solution, complete dissolution of glucosamine prevented the development of supersaturation. As a result, nucleation could not proceed, and no crystal growth was observed. Since crystallization equilibrium can only be reached when the mother liquor becomes saturated, the unsaturated solution was unable to produce crystals.

International Journal of Applied Science and Engineering Review

IJASER

ISSN: 2582-6271

Vol. 6, Issue.6, Nov-Dec 2025, page no. 64-74

3.2 Effect of Cooling Temperature on the Purification of Glucosamine Solution through Cooling Crystallization

Figure 2 presents the yield profile as a function of cooling time at temperatures of 25 °C and 0 °C. The results show that the yield obtained at 0 °C was consistently higher than that at 25 °C, with the highest yield achieved at 0 °C after 6 hours of cooling. This trend indicates that lower temperatures more effectively promote the generation of supersaturation, which is a key driving force for crystal formation [11], [12].

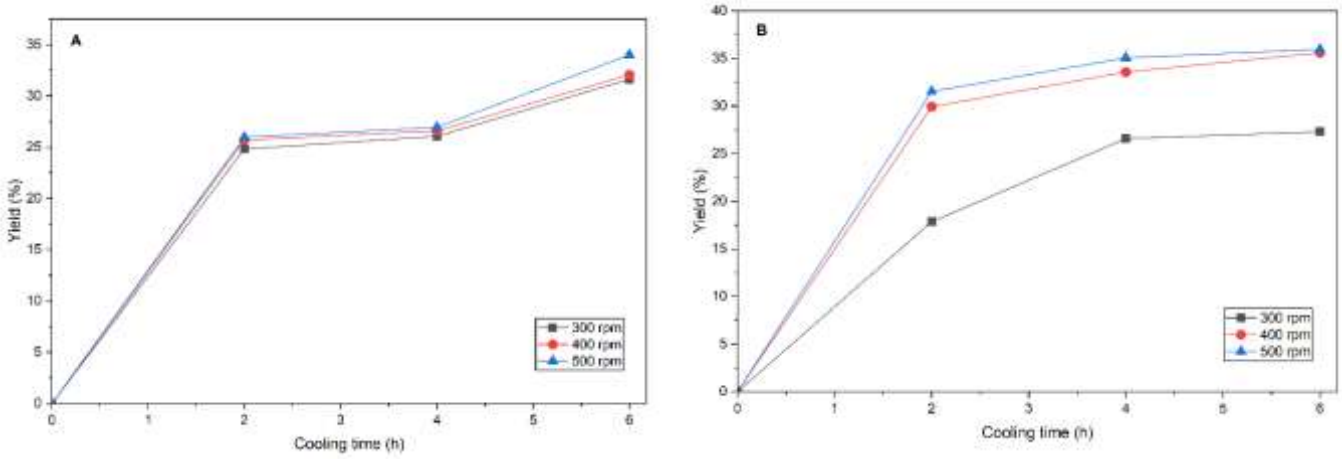

Figure 2: Yield profile as a function of cooling time at different stirring speeds: (a) 25 °C and (b) 0 °C.

Supersaturation can be generated through four primary mechanisms: temperature reduction, solvent evaporation, chemical reaction, and changes in solvent composition. In cooling crystallization, supersaturation is achieved by lowering the temperature of a saturated solution, which decreases the solubility of the solute and drives the system into a supersaturated state where nucleation and crystal growth can occur [13]. A greater temperature difference between the saturation stage and the cooling stage enhances this effect, resulting in a larger driving force for crystallization.

Crystallization is a stochastic process influenced by multiple factors, including impurities, additives, mixing intensity, heat transfer efficiency, and material properties [14]. Nevertheless, the results clearly demonstrate that cooling at 0 °C produced significantly higher yields than cooling at 25 °C, primarily due to the larger temperature gradient, which led to a stronger supersaturation driving force and consequently more extensive crystal formation.

ISSN: 2582-6271

Vol. 6, Issue.6, Nov-Dec 2025, page no. 64-74

3.3 Effect of Stirring Speed on Crystal Formation in the Crystallization Process

From Figure 2, it can be observed that the stirring speed influences the characteristics of the crystals formed. Higher stirring speeds promote increased crystal formation due to enhanced particle–particle interactions, which facilitate agglomeration—the merging of two or more crystal particles into larger structures. Crystallization is also a stochastic process affected by factors such as impurities, additives, mixing intensity, heat transfer, and material properties [14]. Therefore, the higher yield obtained at 500 rpm under cooling conditions of 0 °C can be attributed to more frequent particle collisions that promote nucleation and agglomeration, ultimately resulting in greater crystal formation.

3.4 Surface Morphology

SEM analysis was conducted to compare the surface morphology of raw glucosamine powder with the purified glucosamine crystals. The SEM observations were performed on the raw glucosamine and on the optimal crystallized product obtained at 0 °C and 500 rpm. The SEM images are presented in Figure 4.

International Journal of Applied Science and Engineering Review

IJASER

ISSN: 2582-6271

Vol. 6, Issue.6, Nov-Dec 2025, page no. 64-74

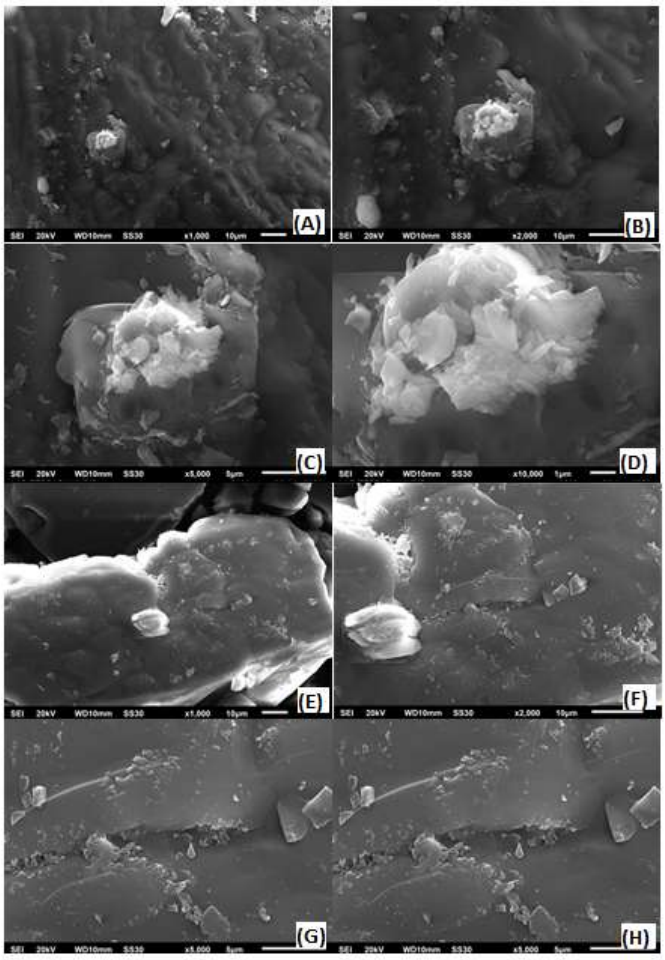

Figure 4: SEM images of glucosamine: (a–d) Raw glucosamine at 1000×, 2000×, 5000×, and 10,000× magnification;

(e–h) Crystallized glucosamine at 1000×, 2000×, 5000×, and 10,000× magnification.

SEM images of the raw material (Figures 4a–4d) show that the glucosamine surface consists of irregular clusters or aggregates with loose and uneven morphology, which is characteristic of powdered solids. In contrast, the SEM images of the purified glucosamine crystals (Figures 4e–4h) exhibit smoother and denser surface morphology. These observations indicate that the powder material has undergone structural transformation into a more compact crystalline form.

International Journal of Applied Science and Engineering Review

IJASER

ISSN: 2582-6271

Vol. 6, Issue.6, Nov-Dec 2025, page no. 64-74

3.5 Chemical Structure

The FTIR spectrum was used to identify the characteristic functional groups of glucosamine within the mid-infrared region (4000–400 cm^{-1}). The FTIR profiles of raw and crystallized glucosamine are presented in Figure 5.

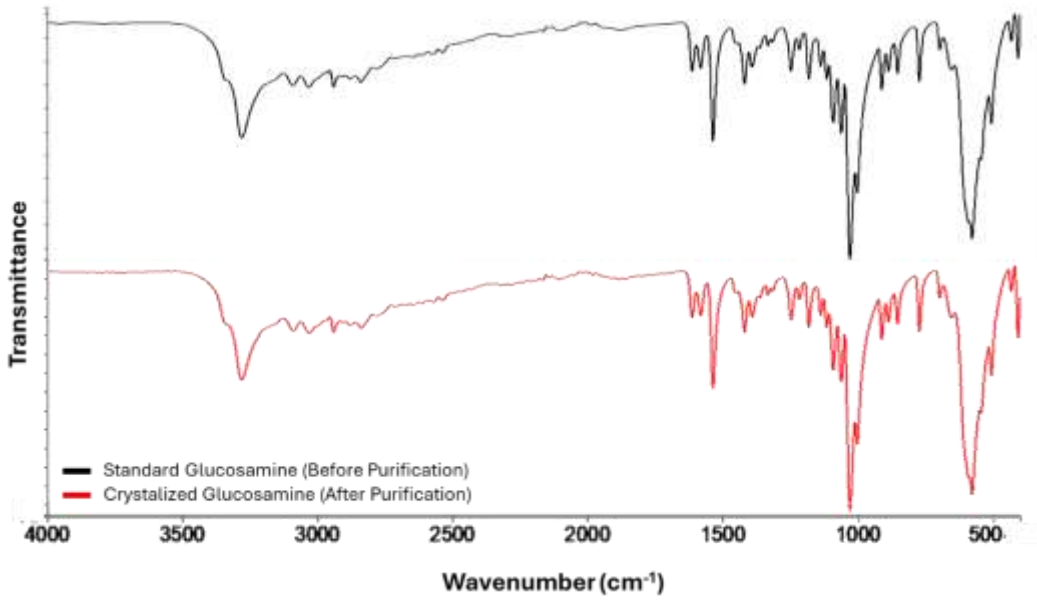

Figure 5: FTIR spectra of glucosamine before and after crystallization.

As shown in Figure 5, both samples exhibit absorption bands corresponding to key functional groups of glucosamine. The crystallized product displays an O–H stretching band at 3283 cm^{-1}, an N–H bending vibration at 1657.97 cm^{-1}, and a C–N stretching band at 1154.28 cm^{-1}. These values align with those reported in the literature, where glucosamine typically shows O–H, N–H, and C–N bands at 3359.95 cm^{-1}, 1614.37 cm^{-1}, and 1321.19 cm^{-1}, respectively [15]. The similarity of these vibrational signatures confirms that the fundamental chemical structure of glucosamine remains preserved after the crystallization process.

3.6 Purity Assessment

HPLC analysis was performed to evaluate the purity of glucosamine by comparing the chromatographic profiles of the raw material and the crystallized product. The chromatograms for both samples are presented in Figure 6.

International Journal of Applied Science and Engineering Review

IJASER

ISSN: 2582-6271

Vol. 6, Issue.6, Nov-Dec 2025, page no. 64-74

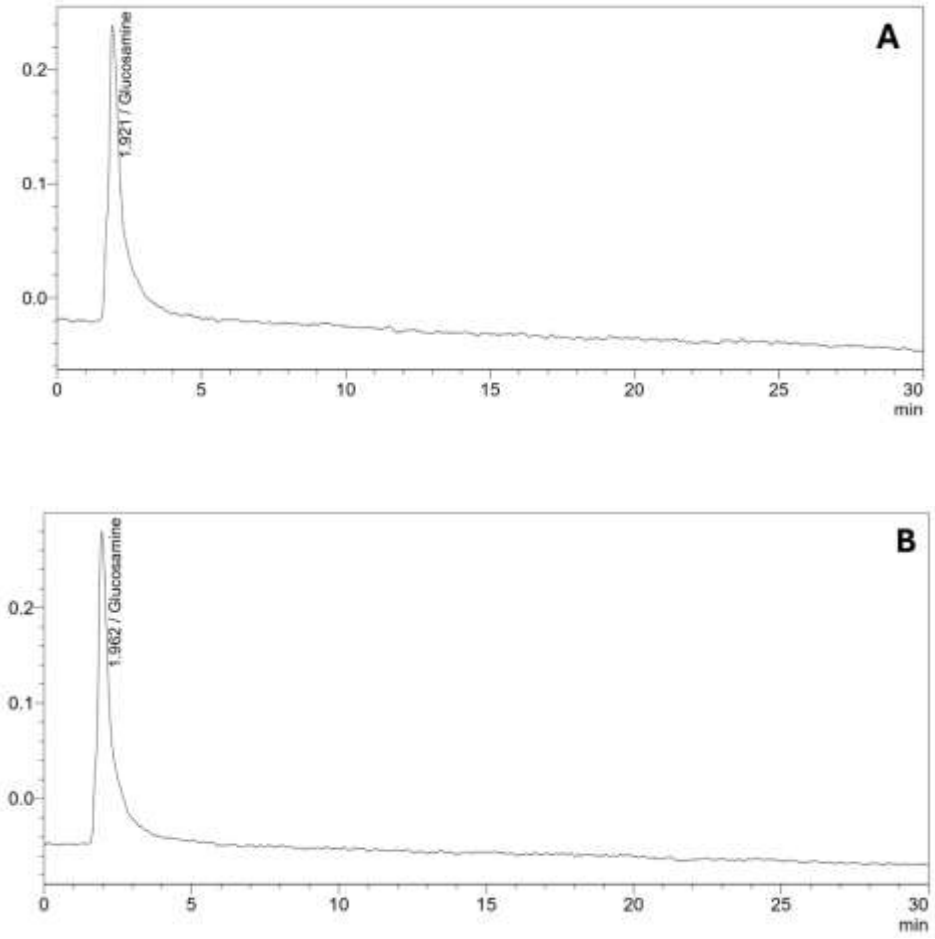

Figure 6: HPLC chromatograms: (a) standard glucosamine (before purification) and (b) crystallized glucosamine (after purification).

As shown in Figure 6, the standard glucosamine exhibits a retention time of 1.921 minutes. The crystallized glucosamine shows a retention time of 1.962 minutes, which is in close proximity to the standard value. This similarity indicates that the cooling crystallization process effectively enhances glucosamine purity, yielding a product with chromatographic characteristics consistent with high-purity glucosamine.

4. CONCLUSIONS

This study confirms that cooling crystallization is an effective technique for purifying glucosamine. Crystal formation occurred only under supersaturated conditions, while unsaturated solutions did not produce crystals due to the absence of a supersaturation driving force. The optimal operating conditions

ISSN: 2582-6271

Vol. 6, Issue.6, Nov-Dec 2025, page no. 64-74

were identified at 0 °C, 500 rpm, and a cooling time of 6 h, which yielded the highest amount of crystallized product. SEM analysis showed that purified glucosamine exhibited a smoother, denser, and more compact morphology than the raw material. FTIR spectra confirmed the presence of characteristic O–H, N–H, and C–N functional groups at 3283 cm^{-1}, 1657.97 cm^{-1}, and 1154.28 cm^{-1}, respectively. HPLC results further demonstrated that the retention time of the crystallized glucosamine (1.962 min) closely matched that of the standard (1.921 min), indicating that the process produced glucosamine of high purity.

REFERENCES

[1] Q. Ma and X. Gao, "Categories and biomanufacturing methods of glucosamine," *Appl. Microbiol. Biotechnol.*, vol. 103, pp. 7883–7889, 2019.

[2] Q. Ma *et al.*, "Highly E ffi cient Production of N - Acetyl-glucosamine in Escherichia coli by Appropriate Catabolic Division of Labor in the Utilization of Mixed Glycerol/Glucose Carbon Sources," *J. Agric. Food Chem.*, vol. 69, pp. 5866–5975, 2021, doi: 10.1021/acs.jafc.1c01513.

[3] I. D. Puspita, "Bioproduction of Chitin Hydrolysate Containing N- Acetylglucosamine by Serratia marcescens PT6 Crude Chitinase and Its Effects on Bacterial Growth Inhibition in Various Temperature," *ASEAN J. Chem. Eng.*, vol. 23, no. 1, pp. 1–13, 2023, doi: 10.22146/ajche.69794.

[4] S. Wu, "Preparation of water soluble chitosan by hydrolysis with commercial α-amylase containing chitosanase activity.pdf," *Food Chem.*, vol. 128, pp. 769–722, 2011.

[5] S. Pan, S. Wu, and J. Kim, "Preparation of glucosamine by hydrolysis of chitosan with commercial α -amylase and glucoamylase," *J. Zhejiang Univ. B (Biomedicine Biotechnol.*, vol. 12, no. 11, pp. 931–934, 2011, doi: 10.1631/jzus.B1100065.

[6] M. Srabovic, M. Huremovic, and B. Catovic, "Design synthesis and crystallization of acetaminophen," *J. Chem. , Biol. Phys. Sci.*, vol. 7, no. 1, pp. 218–230, 2017.

[7] P. P. Elenska and I. L. Dimitrov, "Influence of rapid cooling on crystal nucleation in lysozyme crystallization solutions of low supersaturation," 2021, doi: 10.1080/01411594.2021.1987431.

[8] T. Zhang, B. Nagy, B. Szilágyi, J. Gong, and Z. K. Nagy, "Simulation and experimental investigation of a novel supersaturation feedback control strategy for cooling crystallization in semi-batch implementation," *Chem. Eng. Sci.*, vol. 225, p. 115807, 2020, doi: 10.1016/j.ces.2020.115807.

[9] J. Wang, W. Cao, L. Zhu, J. Wang, and R. Lakerveld, "Emulsion-assisted cooling crystallization of ibuprofen," *Chem. Eng. Sci.*, vol. 226, p. 115861, 2020, doi: 10.1016/j.ces.2020.115861.

[10] L. Aspillaga, D. J. Bautista, S. N. Daluz, K. Hernandez, J. A. Renta, and E. C. R. Lopez, "Nucleation and Crystal Growth : Recent Advances and Future Trends †," *Eng. Proc.*, vol. 56, no. 1, p. 22, 2023.

[11] M. Pourmohammad and A. Ghadi, "Investigation of Induction Time and Nucleation Kinetics in Sodium Nitrate Nanoparticles : The Role of Super-Saturation and Surfactant Additives," *Iran. J.*

ISSN: 2582-6271

Vol. 6, Issue.6, Nov-Dec 2025, page no. 64-74

Chem. Chem. Eng., vol. 44, no. 03, pp. 632–641, 2025.

[12] J. McGinty, N. Yazdanpanah, C. Price, J. H. ter Horst, and J. Sefcik, "Nucleation and Crystal Growth in Continuous Crystallization," in *The Handbook of Continuous Crystallization*, The Royal Society of Chemistry, 2020, pp. 1–50. doi: 10.1039/9781788012140-00001.

[13] S. Y. Misyura, "International Journal of Thermal Sciences Different modes of heat transfer and crystallization in a drop of NaCl solution : The influence of key factors on the crystallization rate and the heat transfer coefficient," *Int. J. Therm. Sci.*, vol. 159, no. June 2019, p. 106602, 2021, doi: 10.1016/j.ijthermalsci.2020.106602.

[14] M. N. Hussain, J. Jordens, J. J. John, L. Braeken, and T. Van Gerven, "Ultrasonics - Sonochemistry Enhancing pharmaceutical crystallization in a fl ow crystallizer with ultrasound : Anti-solvent crystallization," *Ultrason. - Sonochemistry*, vol. 59, p. 104743, 2019, doi: 10.1016/j.ultsonch.2019.104743.

[15] N. Rokhati, T. D. Kusworo, H. Susanto, and I. N. Widiasa, "Preparation of glucosamine by acid hydrolysis of chitin under microwave irradiation," *AIP Conf. Proc.*, vol. 2197, p. 070001, 2020.